Genetic analyses of undifferentiated small round cell sarcoma identifies a novel sarcoma subtype with a recurrent CRTC1-SS18 gene fusion

Abdullah Alholle[1†], Marie Karanian[2,3†], Anna T Brini[4‡] , Mark R Morris[5‡], Vinodh Kannappan[5], Stefania Niada[4] , Angela Niblett[6], Dominique Ranchère-Vince[2], Daniel Pissaloux[2,3], Christophe Delfour[7], Aurelie Maran-Gonzalez[8], Cristina R Antonescu[9], Vaiyapuri Sumathi[6§*], Franck Tirode[3,10§*] and Farida Latif[1§*]

1 Institute of Cancer and Genomic Sciences, University of Birmingham, Birmingham, UK
2 Department of Biopathology, Centre Léon Bérard, Lyon, France
3 University of Lyon, Université Claude Bernard Lyon 1, CNRS 5286, INSERM U1052, Cancer Research Centre of Lyon, Lyon, France
4 IRCCS Galeazzi, Department of Biomedical, Surgical and Dental Sciences, University of Milan, Milan, Italy
5 Research Institute in Healthcare Science, Faculty of Science and Engineering, University of Wolverhampton, Wolverhampton, UK
6 Department of Musculoskeletal Pathology, The Royal Orthopaedic Hospital, Robert Aitken Institute of Clinical Research, University of Birmingham, Birmingham, UK
7 Anatomy and Pathological Cytology Department, Centre Hospitalo-Universitaire Gui de Chauliac, Montpellier, France
8 Anatomy and Pathology Department, Montpellier Cancer Institute, Montpellier, France
9 Department of Pathology, Memorial Sloan Kettering Cancer Center, New York, NY, USA
10 Department of Translational Research and Innovation, Centre Léon Bérard, Lyon, France
*Correspondence to: V Sumathi, Department of Musculoskeletal Pathology, The Royal Orthopaedic Hospital, Robert Aitken Institute of Clinical Research, Vincent Drive, University of Birmingham, Edgbaston, Birmingham B15 2TT, UK. E-mail: vaiyapuri.sumathi@nhs.net; Or F Tirode, Cancer Research Centre of Lyon, INSERM U1052, Centre Léon Bérard, 28 Rue Laënnec, 69373 Lyon Cedex 08, France. E-mail: franck.tirode@lyon.unicancer.fr;
Or F Latif, College of Medical and Dental Sciences, University of Birmingham, Edgbaston, Birmingham B15 2TT, UK. E-mail: f.latif@bham.ac.uk

Keywords: undifferentiated small round cell sarcoma; Ewing sarcoma; RNA-seq; gene fusion

Received 20 September 2017; Revised 2 February 2018; Accepted 8 March 2018
No conflicts of interest were declared.

Abstract

In recent years, undifferentiated small round cell sarcomas (USRCSs) have been divided into a variety of new, rare, sarcoma subtypes, including the group of Ewing-like sarcomas, which have the morphological appearance of Ewing

sarcomas, but carry CIC –DUX4, BCOR –CCNB3 and other gene fusions different from the classic EWSR1–ETS gene fusion. Using high-throughput RNA-sequencing (RNA-seq) analyses, we identified a novel recurrent gene fusion, CRTC1–SS18, in two cases of USRCS that lacked any known translocation. RNA-seq results were confirmed by reverse transcription polymerase chain reaction, long-range polymerase chain reaction, and fluorescence in situ hybridization. In vitro, we showed that the cells expressing the gene fusion were morphologically distinct and had enhanced oncogenic potential as compared with control cells. Expression profile comparisons with tumours of other sarcoma subtypes demonstrated that both cases clustered close to EWSR1–CREB1-positive tumours. Moreover, these analyses indicated enhanced NTRK1 expression in CRTC1 –SS18-positive tumours. We conclude that the novel gene fusion identified in this study adds a new subtype to the USRCSs with unique gene signatures, and may be of therapeutic relevance.

Diagnosing small round blue cell tumours on biopsy has been challenging because of their lack of specific features in small specimens. Among undifferentiated small round cell sarcomas (USRCSs), Ewing-like sarcoma (ELS) shares some of the morphological features of Ewing sarcoma (ES), but lacks the classic EWSR1–ETS gene fusion [1,2]. ESs are mainly characterized by chromosomal translocations at chromosome 22q12 that fuse EWSR1 with one of the ETS gene family of transcription factors, such as FLI1 or ERG, in 90–95% of ES cases. The classic ES gene fusion protein acts as an oncoprotein, and plays an essential role in tumourigenesis and proliferation of ES cells [2]. Recent studies have identified recurrent gene fusions in ELS, namely CIC–DUX4 and BCOR–CCNB3 [3–6]. The identification of these gene fusions suggests that other, as yet to be identified, gene fusions could be associated with this type of tumour. Furthermore, novel gene fusions in ELS have been reported recently in case reports, including CIC–FOXO4, BCOR–MAML3,andZC3H7B–BCOR [7–9]. Identifying these genetically defined entities may contribute towards understanding the pathogenesis and the behaviour of these tumours.
By applying RNA sequencing (RNA-seq) technology to investigate USRCS, we discovered a novel CRTC1–SS18 gene fusion in two samples from two different cancer centres. Combining both samples, we were able to find similarities at the clinical, patholog-ical, and molecular levels. Moreover, by cloning the fusion gene we were able to demonstrate its oncogenic properties, adding the CRTC1–SS18 fusion gene to the increasing number of described oncogenes.

Materials and methods

One patient sample (case 1) was obtained from the Royal Orthopaedic Hospital NHS Foundation Trust Tumour Bank (with permission; REC 12/EM/0048). The other patient sample (case 2) was obtained from resection material sent to the Centre Léon Bérard for molecular diagnosis. Both samples were acquired with informed consent from the patient and or/next of kin, and ethical approval from institutional and local research commit-tee boards. Patient samples were anonymized and used in accordance with the principles expressed in the Declaration of Helsinki.

Immunohistochemistry

Case 1

For immunohistochemistry, 2-µm-thick sections were cut, and antigens were retrieved in an epitope retrieval solution of pH 8 (RE7116; Novocastra, Newcastle upon Tyne, UK) at 68 ∘C for 17 h in a stirred water bath. The antibody clones, dilutions and sources were as follows: anti-CD99 (12E7, 1:25; Dako, Ely, UK), anti-vimentin (V9, 1:100; Novocastra), anti-CD31 (JC70, 1:100; Dako), anti-CD34 (QBend10, 1:50; Dako), anti-cytokeratin AE1/AE3 (1:100;
Dako), anti-CD45 (2B11 + PD7/26, 1:200; Dako), anti-cytokeratin MNF116 (1:50; Dako), anti-desmin
(D33, 1:100; Dako), anti-α-smooth muscle actin (SMA)(1A4, 1:200; Dako), anti-epithelial membrane anti-gen (EMA) (E29, 1:100; Dako), anti-HMB45 (1:200; Dako), anti-S100 (NCL-L-S100p, 1:1000; Novo-castra), anti-Wilms tumour 1 (WT1) (C-19, 1:500; Santa Cruz, Insight Biotechnology Limited, Wembley, UK), anti-TLE1 (M-101, 1:50; Santa Cruz), anti-ERG (Erg-1/2/3 C-1, 1:50; Santa Cruz), anti-INI1 [1:25; BD Transduction Laboratories (BD Biosciences), Becton Dickinson UK, Oxford, UK], anti-BCOR (C-10, 1:50; Santa Cruz), anti-ETV4 (16, 1:50; Santa Cruz), and anti-Ki67 (MIB1, 1:200; Dako).

Case 2

Sections were cut at a thickness of 4 µm from formalin-fixed paraffin-embedded (FFPE) tissue, and immunostained with a VentanaBenchmark XT automatic stainer (Ventana, Tuscon, AZ, USA). Sig-nals were revealed with the ultraView Universal Dab Detection kit (Ventana). The following antibodies were used: anti-CD99 (12E7; Dako), anti-EMA (E29, 1:50; Dako), anti-desmin (D33, 1:80; Dako), anti-cytokeratin AE1/AE3 (AE1/AE3, 1:50; Dako), anti-caldesmon (h-CD, 1:100; Dako), anti-myogenin (F5D, 1:100; Dako), anti-S100 (Z0311, 1:800; Dako), anti-CD34 (QBend-10, 1:25; Dako), anti-INI1 (25, 1:50; BD Transduction Laboratories), anti-BCOR (C-10, 1:50; Santa Cruz), and anti-ETV4 (16, 1:50; Santa Cruz). Immunohistochemistry for neurotrophic receptor tyro-sine kinase 1 (NTRK1) was performed with a 32-min incubation with the anti-NTRK1 antibody (ab76291, clot EP1058Y, dilution 1:200; Abcam, Cambridge, UK) on a Ventana ULTRA machine with Cell Conditioning Solution 1 pretreatment for 64 min.

Fluorescence in situ hybridization (FISH) analyses

FISH analyses were performed on FFPE tissue sections with the ZytoLight SS18 Dual Color Break Apart Probe (#Z-2097-200; Zytovision, Bremerhaven, Germany) by assessment of at least 100 non-overlapping intact nuclei by two independent operators. The positive threshold for calling the FISH assay positive was 15%.

Array-comparative genomic hybridization (aCGH) analyses

Genomic DNA was extracted from FFPE tissue with a QIAamp DNA micro kit (Qiagen, Hilden, Germany). Genomic DNA and human reference DNA (Promega, Madison, WI, USA) were labelled with cyanine 5 and cyanine 3, respectively, by use of the Genomic DNA High-Throughput ULS Labeling Kit (Agilent Technologies, Santa Clara, CA, USA), and co-hybridized onto a 4x180K Sureprint G3 Human CGH microarray (Agilent Technologies), according to the manufacturer's recommendations. Data were analysed with Agilent Genomic Workbench

software v7.0 or with Cytogenomics software (v2.9.2.4; Agilent), and expressed according to the human reference genome hg19 (GRCh37; Genome Reference Consortium Human Reference 37). The identification of aberrant copy number segments was based on the ADM-2 segmentation algorithm with a threshold of 6.0.

Fresh frozen tissue RNA-seq

Total RNA was extracted from fresh frozen tissue (case 1) with a Qiagen RNeasy Mini kit (Qiagen, Hilden, Germany) according to the manufacturer's protocol. RNA quality and quantity were measured with an Agilent 2100 bioanalyzer (Agilent Technologies). An RNA sample was sent to Oxford Gene Technology (Begbroke, UK) for performance of RNA-seq with the Illumina HiSeq 2000 platform (Illumina, San Diego, CA, USA). In brief, cDNA libraries were prepared from

1 µg of total RNA with the Illumina TruSeq RNA Sam-ple Prep Kit v2. All sequencing was paired-end (100 bp) and performed over 100 cycles, and the read files (Fastq) were generated from the sequencing platform via the manufacturer's software. Mapping and alignment were processed with the Tuxedo suit. The human sequence genome (hg19) was used as a reference and aligned to the sequence reads. Fusion Catcher software was used to identify gene fusions from RNA-seq data [10]. RNA-seq data have been deposited (SRA accession: SRP131744).

FFPE RNA sequencing

RNA was extracted from FFPE tissue sections (case 1 and case 2) with Trizol reagent (Thermo Fisher Scien-tific, Courtaboeuf, France), and subsequently extracted with phenol/chloroform. The RNase-free DNase Set (Qiagen, Courtabouef, France) was used to remove DNA. The DNase was eliminated by a further Trizol extraction. All RNAs were quantified by spectrophotom-etry (NanoDrop; Thermo Fisher Scientific), and qual-

ity was controlled (DV200 value cutoff of >13%) by use of a TapeStation with Hs RNA ScreenTape (Agi-lent Technologies). One hundred nanograms of total RNA was used to prepare a library with a TruSeq RNA Access Library Prep Kit (Illumina). Fourteen libraries were pooled at 4 nM with 1% PhiX as an internal control. Sequencing was performed (75 cycles, paired end) with a NextSeq 500/550 High Output V2 kit and an Illumina NextSeq 500 (Illumina). Align-ments were performed with the STAR algorithm [11] against the GRCh38 reference genome, and fusion gene assessments were made with STAR-Fusion [12], Fusion-Catcher [10] and FusionMap [13] tools. Expression pro-files were extracted from fastq files with Kallisto [14],

and transformed as log2(TPM + 2) prior to quantile normalization with the Limma package v 3.32.2 per-formed in the R environment v3.4.1 [15]. Only genes with a coding sequence annotation (based on Ensembl GRCh38p5 annotation) and with a maximum expression

value across all samples of >2wereconsideredforthe clustering analysis, which was performed by the use of Ward's distance on the 10% most variant genes based on their interquartile range. RNA-seq data have been deposited (SRA accession: SRP131744).

Reverse transcription polymerase chain reaction (RT-PCR) and Sanger sequencing

cDNA was generated from total RNA with Super-Script III (Invitrogen) and random primers (Promega). The RT-PCR reactions were performed withy 2.5 µl of 10X buffer, 2.5 µl of dNTPs (2.5 mM), 5 µlof5X GC-rich solution, 1 µl of forward primer (20 pmol), 1 µl of reverse primer (20 pmol), and 0.1 µlofFastStart DNA polymerase (Roche, Burgess Hill, UK). Primer sets used for polymerase chain reaction (PCR) amplification were CRTC1-F (TCGAACAATCCGCGGAAATT) and SS18-R (GTGCTGGTAAAAGAGACTGCA), and PCR products were visualized with 2% (w/v) agarose gel (Bioline, London, UK). The PCR products were extracted from the gel and purified with a QIAquick Gel Extraction Kit (Qiagen, Hilden, Germany). A BigDye Terminator V3.1 kit (Applied Biosystems, Foster city, CA, USA) was used for the cycle sequencing reaction, and PCR products of CRTC1-SS18 gene fusions were directly Sanger sequenced with an ABI 3730 DNA analyser (Applied Biosystems).

Long-range PCR (LR-PCR)

LR-PCR was carried out with PrimeSTAR GXL DNA polymerase (Takara Bio, Shiga, Japan). Each LR-PCR reaction was set up with 50 ng of DNA, 1 × 5X PrimeS-TAR GXL buffer, 200 µM each dNTP, 0.2 µM forward primer, 0.2 µM reverse primer, and 1.25 U of PrimeS-TAR GXL DNA polymerase enzyme, made up to a
final volume of 50 µlwithsterilized distilled water.

The PCR was carried out with the following condi-tions: 30 cycles of 10 s at 98 ∘Cand10minat60∘C. The LR-PCR primers used in this study are listed in supplementary material, Table S1. The size of the PCR product from the gene fusion was unknown; therefore, genome walking through both genes and a rough esti-mation of the product size was carried out. The genome walking covered the exonic and intronic regions of both genes involved in the fusion. LR-PCR was performed on the genomic DNA of the tumour sample. One for-ward primer (F3) was anchored on exon 1 of CRTC1,and
different reverse primers spanning ∼2.5 kbp of intron 1wereused to amplify this region and to identify the breakpoint. The samples were electrophoresed on 0.9%agarose gels to determine the size of the PCR product. After confirming the breakpoint of CRTC1–SS18 gene fusion at the genomic level, LR-PCR was per-formed on both the tumour sample and the corresponding normal tissue to confirm that this fusion was somatic. The PCR product was then extracted from the gel and sequenced.

Plasmid construction

The CRTC1–SS18 expression construct was made by PCR amplification of the entire fusion construct with the cDNA generated from case 1 tumour RNA. This amplicon was subcloned into the expression vector pFlag-CMV-4 (Sigma-Aldrich, Dorset, England) by the use of EcoRI and XbaI restriction sites. The primers used were as follows: forward, 5′ -cg g aat tcg aag atg gcg act tcg aac aat c-3 ;and reverse ,5′ -cg tctaga t tca ctg ctg gta att tcc ata c-3. Plasmid constructs were verified by sequencing. Expression of this plasmid generates an N-terminal FLAG-tagged protein. The construct plasmid and associated empty vector were transfected into HEK293 cells (ATCC, Manassas, VA, USA), clones were isolated, and expression was validated by western blotting with an anti-FLAG antibody (Cat. No. F1804, clone M2, 1:1000; Sigma-Aldrich). Clones were maintained in

Dulbecco's modified Eagle's medium (DMEM) and 10% fetal bovine serum (FBS) supplemented with 1 mg/ml G418 (Life Technologies, Carlsbad, CA, USA).
Cell migration assays
Suspensions containing 25 000 cells of a stable CRTC1–SS18-expressing HEK293 clone, or a clone containing the empty vector, suspended in serum-free DMEM were seeded into a 24-well format Boyden
chamber cell culture insert (8-μmporesize; PET membrane) (BD Falcon, Bedford, MA, USA). The lower chamber contained DMEM, and 10% FBS as an attractant. Chambers were incubated for 16 h. Cells were fixed in methanol; cells on the upper side of the chamber were removed, and those remaining on the underside were stained with crystal violet. Migrated cells were photographed, the crystal violet was solubilized in 500 μl of 33%acetic acid, and the optical density was measured at 540 nm (n = 20).

Cell invasion assays
Amodified migration assay was carried out in which 50 000 cells were seeded into Boyden chambers (8-μmpore size; PET membrane) (BD Falcon) pre-coated with 100 μl of Geltrex basement membrane matrix (Thermo Fisher Scientific). Chambers were incubated for 16 h. Invasive cells were counted by microscopy with the observer unaware of the cell type (n = 22).

Soft agar, anchorage-independent growth assay
Anchorage-independent growth in soft agar was assessed with the CytoSelect 96-Well Cell Transforma-tion Assay kit (Cell Biolabs, San Diego, CA, USA), according to the manufacturer's instructions. In brief, 2500 cells per well were seeded in agar supplemented with DMEM and 10% FBS. Following incubation for 8days, the agar was solubilized and viable cells were lysed, stained and quantified by fluorometry (excitation 492 nm, emission 520 nm; n = 8).

Results
Clinical presentation and pathological findings of the index case, case 1
Clinical presentation
A35-year-old man presented to the Royal Orthopaedic Hospital with a rapidly growing lump on his right thigh.
Magnetic resonance imaging revealed a heterogeneous mass within the sartorius muscle, and the findings were in keeping with a soft tissue sarcoma. A diagnosis of USRCS was made on the biopsy material of the tumour, which did not carry the chimeric gene fusions associated with ES (EWSR1–FLI1 or EWSR1–ERG), mesenchymal chondrosarcoma (EWS–NR4A3 and TAF2N–NR4A3), DSRCT (EWS–WT1), or synovial sarcoma (SS) (SS18–SSX). The tumour was also neg-ative for CIC–DUX4 and BCOR–CCNB3. In view of this diagnosis, the patient received four cycles of vincristine, ifosfamide, doxorubicin and etoposide. Radiologically, there was no response to chemotherapy, and the mass was excised. The patient developed bilat-eral lung metastases 18 months after diagnosis, and died of disease 92 months later.
Pathological findings
Grossly, an intramuscular, well-circumscribed greyish white fleshy tumour with haemorrhagic and necrotic foci

measuring 7 × 65 × 53 mm was observed (Figure 1A). Histologically, the tumour consisted of solid sheets and nests of small round cells surrounded by desmoplastic stroma reminiscent of desmoplastic small round cell tumour (DSRCT). The tumour cells had scant amounts of eosinophilic cytoplasm and small, irregularly shaped round nuclei with stippled chromatin. Some had prominent grooves and small nucleoli. Focal areas of necrosis and mitotic figures were identified (seven per 10 high-power fields). Rosette formation and glandular differentiation were not identified (Figure 1B,C). Immunohistochemically, the tumour cells were diffusely positive for vimentin and CD99 (Figure 1D). The tumour cells did not stain for CD31, CD34, AE1/AE3, CD45, CK(MNF116), desmin, EMA, HMB45, SMA, S100, HMB45, WT1, TLE1, ERG, ETV4, BCOR, or CCNB3. INI1 expression was retained. The Ki67 labelling index was up to 20%.

RNA-seq analysis and confirmation of gene fusion

RNA-seq analysis of the index case (case 1) revealed anovelgene fusioninvolvingCRTC1 and SS18 in the tumour sample. Two alternative splicing fusion tran-scripts were detected that linked exon 1 of CRTC1 with exon 2 or exon 3 of SS18 (Figure 2A,B; supplementary material, Figure S1). A balanced translocation resulted in SS18 being fused with exon 1 of CRTC1, generating an in-frame fusion protein (Figures 2A,B and 4A). The CRTC1–SS18 fusion transcripts were confirmed by RT-PCR and Sanger sequencing (Figure 2B; supple-mentary material, Figure S2A). In order to map the fusion breakpoints at the genomic level, LR-PCR was carried out to reveal the genomic sequence around the breakpoints (supplementary material, Figure S2B–D and Table S1). The CRTC1 breakpoint was found to be 8bp from the 3′ -end of exon 1 (cDNA fusion point), and the SS18 breakpoint was 4457 bp before the 5′ -end of exon 1 (Figure 2C).

Clinical presentation and pathological findings of case 2

Clinical presentation

RNA sequencing revealed a second case of an CRTC1–SS18-positive USRCS (case 2): a 42-year-old woman who presented to the CHU Gui de Chauliac (Montpellier, France) with a mass from the popliteal fossa, later diagnosed as an undifferentiated small cell sarcoma. The patient underwent radiotherapy and chemotherapy prior to the surgical removal of the tumour. A tumour fragment was sent to the Centre Léon Bérard's department of pathology for a second opinion and molecular diagnosis.

Pathological findings

An intramuscular mass, well circumscribed by a diffuse
calcified matrix, measuring 110 × 75 × 70 mm was observed. The tumour consisted of bundles and nests of cells embedded in a focally myxoid fibrous stroma (Figure 3A). There were areas of necrosis. Cytologically, the tumour was composed of oval to epithelioid cells (Figure 3B). The cells were of medium size with abundant eosinophilic cytoplasm and ovoid and vesicular nuclei with nucleoli (Figure 3C). Immunohistochemically, the tumour cells were positive for CD99 and negative for keratins, EMA, desmin, caldesmon, myogenin, S100, CD34, ETV4, and BCOR. INI1 expression was retained. NTRK1 was diffusely positive. RNA-seq performed on the FFPE material showed an in-frame fusion between

exon 1 of CRTC1 and exon 2 of SS18. In this case, the translocation was unbalanced, as demonstrated by FISH (Figures 2A and 4A). It is of note that the cell morphology was similar in the tumour biopsy acquired before treatment, which also harboured the CRTC1–SS18 fusion gene.

Genomic and transcript profiles

aCGH analyses revealed that case 1 had a diploid genome and a balanced CRTC1–SS18 translocation, whereas case 2 had a tetraploid genome with an unbalanced CRTC1–SS18 translocation (see Figure 4B for specific chromosomal gains and losses for each case). To enable comparison of both samples, RNA-seq of case 1 was also performed on an FFPE sample, in the same pipeline as case 2. Hierarchical clustering analysis (of RNA-seq data) demonstrated that both samples clustered together and close to the EWSR1–CREB1-positive tumours but not with ESs or ELSs (Figure 4C). Also, CRCT1–SS18-positive samples did not cluster with the recently described cutaneous melanocytomas harbouring a CRTC1–TRIM11 fusion gene [16]. Furthermore, RNA-seq data revealed enhanced NTRK1 expression in the two cases with the CRTC1–SS18 gene fusion as compared with other sarcomas with known translocations such as EWSR1–CREB1, BCOR–CCNB3, CIC–DUX4,and EWSR1–FLI1 (Figure 4D), and this was confirmed at the protein level by immunohistochemistry (supplementary material, Figure S3).

Functional analysis of the CRTC1–SS18 gene fusion product

To determine whether the product of the CRTC1–SS18 gene fusion identified had any potential oncogenic activity, the fusion gene from case 1 was cloned into a tagged mammalian expression vector, and human HEK293 clones expressing the construct were generated; a fusion protein of the predicted size
(~57 kDa) was observed (supplementary material, Figure S4). The CRTC1–SS18-positive clone were morphologically distinct from control clones, showing extended pseudopodia and pronounced intracytoplasmic vacuoles (Figure 5A). We proceeded to assess the anchorage-independent growth potential of these cells (hallmark of transformation). CRTC1–SS18-expressing HEK293 cells were seeded into semisolid agar, in 96-well microtitre plates, and incubated for 8 days. The number of viable cells was then determined with a commercial fluorescence assay. Following this relatively short period of incubation, the assay indicated that there were 3.7 times the number of viable cells expressing CRTC1–SS18 as control HEK293 cells transfected with an empty plasmid. This increase in the number of viable cells was statistically significant (Figure 5B). As expression of this fusion protein appeared to increase anchorage-independent growth, we continued to assess these cells for other hallmarks of malignancy. We carried out assays to determine the migratory and invasive potential of the CRTC1–SS18-expressing cells. In a Boyden chamber assay, in which cells are
encouraged to pass through 8-μmpores, significantly more HEK293 cells expressing CRTC1–SS18 migrated than control cells; this was determined both visu-ally and with a colourimetric assay (Figure 5C). In a similar assay, in which the membranes of the cham-bers are coated in a basement membrane matrix to model the invasive potential of these cells, 2.6 times more CRTC1–SS18-expressing cells than control cells invaded through the membrane in a 16-h period (Figure 5D).

Discussion

ELS or USRCS is a subtype of small blue round cell tumour that has a morphological appearance close to that of ES but lacks the characteristic EWSR1–ETS gene fusion. Recently, some of these USRCSs have been shown to carry gene fusions involving CIC–DUX4, CIC–FOXO4, BCOR–CCNB3, BCOR–MAML3,and ZC3H7B–BCOR [3–8]. In this study, we have identified, by RNA-seq, a novel recurrent CRTC1–SS18 gene fusion in two USRCSs that were negative for known gene fusions in this sarcoma type. The CREB-regulated transcription coactivator 1 (CRTC1) gene belongs to a family of highly conserved cAMP response element-binding protein (CREB) coactivators [17,18]. CRTC1 has already been implicated in other translocations, such as the CRTC1–MAML2 fusion in mucoepidermoid carcinoma of salivary, bronchial and thyroid glands [19–22], and the CRTC1–TRIM1 fusion in cutaneous melanocytomas [16]. The SS18 protein (NBAF chromatin remodelling complex sub-unit SS18) functions as a transcriptional coactivator, and interacts directly with members of the SWI–SNF chromatin remodelling complex [23]. The SS18–SSX fusion is a result of the chromosomal translocation t(X;18)(p11;q11) in almost all cases of SS, which account for approximately 10–20% of all soft tissue sarcomas [24–26].

These two cases of CRTC1–SS18-positive sarcoma are regarded as a distinct entity from all other ELSs, DSRCTs and poorly differentiated SSs described in the literature. Poorly differentiated SS is characterized by high cellularity, polygonal to small round cell morphology, frequent mitoses, and necrosis. These poorly differentiated SSs may be distinguished by the expression of high molecular weight cytok-eratins and CD99, and having the characteristic t(X;18)(p11:2;q11:2) translocation. However, these two cases of CRTC1–SS18-positive sarcoma had a distinct morphology relative to that seen in poorly differentiated SS, and lacked the characteristic t(X;18)(p11:2;q11:2) translocation. Only one other ELS tumour with a CIC–FOXO4 gene fusion has been described with desmoplastic stroma that showed immunoreactivity for CD99 and focal WT1. This tumour occurred in the neck of an elderly male. DSRCT commonly arises in the abdominal cavity in children and young adults, and is characterized histologically by nests of small round cells surrounded by desmoplastic stroma, immunohistochemically by positive staining for keratins, desmin, and WT1, and genetically by the presence of a recur-rent translocation, i.e. t(11;22)(p13;q12). However, the tumours that we describe here occurred in lower limbs of adult patients, and the tumour cells were larger than cells of DSRCT, with more cytoplasm, and showed immunoreactivity for CD99 but did not carry the EWS–WT1 gene fusion.

Morphologically, the two tumours that we present here shared features: large fibrous stroma, and small to medium cells with eosinophilic cytoplasm and vesicular nuclei. Expression profile analyses confirmed that our CRTC1–SS18-positive sarcomas were not related to ES or ELS, but rather to EWSR1–CREB1-positive tumours. It is of note that CRTC1–TRIM11-positive cutaneous melanocytomas were also found to resemble EWSR1–CREB1-positive clear cell sarcomas [16], but hierarchical clustering clearly separated both types of CRTC1-fused tumours. Finally, we also present here evidence, at both the RNA level and the protein level, that NTRK1 is expressed at higher levels in CRTC1–SS18-positive sarcomas than in other related tumours. We could not find any fusion involving NTRK1 in these tumours, explaining its elevated level Nevertheless,

NTRK1 expression may be useful as a marker for differential diagnosis, but most importantly may be used as a therapeutic target. In addition, we demonstrate that the cells expressing the CRTC1–SS18 gene fusion were morphologically distinctive from control cells and had enhanced oncogenic potential.

In summary, we have presented two cases of USRCS with a novel CRTC1–SS18 gene fusion. It would be beneficial to screen more samples to determine the frequency of CRTC1–SS18 gene fusion in other USRCSs. The severe clinical phenotype (lung metastasis at an early age) of case 1 (case 2 has 6 months of follow-up), the novel CRTC1–SS18 gene fusion and the expression profile data indicate that these tumours may be classified as a new type of USRCS. Except for sporadic and unique cases, to our knowledge the two USRCSs in this study are the only cases of a sarcoma type other than SS involving SS18 as a recurrent gene fusion partner. The discovery of this new fusion should enable better classification and study of these rare sarcomas. CRTC1–SS18-positive sarcoma should be considered in the differential diagnosis of USRCS, DSRCT and poorly differentiated tumours that show SS18 split signals with FISH. Elevated levels of NTRK1 in CRTC1–SS18-positive sarcomas may be of therapeu-tic importance and amenable to treatment with tyrosine kinase inhibitors [27]. Considered all together, for the field of rare to ultra-rare sarcomas, this study offers a nice example of the need to assess samples from different cancer centres to identify recurrent fusions and to be able to characterize new sarcoma subtypes. Further collaboration between groups is therefore required to depict the whole landscape of small round cell sarcomas.

Acknowledgements

This research was funded in part by the Kuwait Med-ical Genetics Centre (KMGC), Ministry of Health, Kuwait, the Royal Orthopaedic Hospital NHS Founda-tion Trust, Birmingham, UK, the Centre Léon Bérard, Lyon, France, the Institut National de la Santé et de la Recherche Médicale, the Italian Ministry of Health (Ricerca Corrente RC L2029, IRCCS Galeazzi Orthopaedic Institute), and the Department of Biomed-ical, Surgical and Dental Sciences, University of Milan (grant number 15-63017000-700).

Author contributions statement

AA, ATB, FT, VS, and FL designed the research and analysed the data. VS, AN, CD, and AMG provided tumour samples. VS and MK reviewed slides and the clinical information. AA, MRM, VK, SN, CA, MK, and DP performed experiments and/or analysed data. AA, ATB, MRM, MK, FT, VS, and FL wrote the paper. All authors approved the final version.

Figure Legends

Figure 1. Macroscopy and microscopy images of case 1. (A) The macroscopic image shows a fairly well-circumscribed fleshy tumour with foci of necrosis and haemorrhage. (B) The microscopic image (low power) shows the tumour to be composed of solid sheets and nests surrounded by desmoplastic stroma. (C) The high-power view of the tumour shows small cells with scant cytoplasm. (D) Membranous staining with CD99, mimicking ES.

Figure 2. RNA-seq identification of the CRTC1–SS18 gene fusion. (A) The genomic intron–exon structure of CRTC1 (blue) and SS18 (red). CRTC1(exon 1)–

SS18(exon 2) gene fusion was found in case 1 and case 2, whereas CRTC1(exon 1)–SS18(exon 3) alternative splicing gene fusion was found only in case 1. (B) A Sanger sequencing chromatogram of the RT-PCR product confirmed the CRTC1(exon 1)–SS18(exon 2) fusion junction and the CRTC1(exon 1)–SS18(exon 3) fusion junction in case 1. (C) Schematic of the exon–intron structure of the CRTC1–SS18 gene fusion at the DNA level. The intergenic breakpoints for both genes are shown, and were confirmed by Sanger sequencing of the LR-PCR product in case 1.

Figure 3. Microscopy images of case 2. (A) Haematoxylin and eosin (HE) (low-power objective, ×10): sheets and nests of cells in desmoplastic stroma. (B) HE (×20): nest of epithelioid cells. (C) HE (objective ×40): cells were of medium size with abundant eosinophilic cytoplasm and ovoid and vesicular nuclei with nucleoli.

Figure 4. Genomic and transcript profiles of CRTC1–SS18-positive sarcomas. (A) FISH analysis with an SS18 break-apart probe, showing multiple copies of chromosome 18 carrying SS18. Most cells were tetrasomic or greater for the SS18 locus on chromosome 19. In case 1, the translocation was balanced (presence of red dots), whereas in case 2 the translocation was unbalanced (the red signal is lost while the green signal remains). (B) aCGH profiles. Case 1 had a diploid genome with the loss of chromosomes 1, 3p, and 9, and parts of 11q, 17p, 18, and 22, together with gains on chromosomes 3q, 5, 6, 7, 9, 10, 11, 16, 17, 20, and 21. The region around SS18 on chromosome 18 was focally gained, whereas the CRTC1 locus was normal, which is in accordance with a balanced translocation. Case 2 had a tetraploid genome with the loss of one copy of chromosomes 1, 3, 13, 14, 17, 21, and 22, and with homozygous deletion of chromosome region 17q22, impacting on MBTD1, UTP18,andCA10.The5′ region of SS18 (on the minus strand) and the 3′ region of CRTC1 (on the plus strand) were lost, in accordance with an unbalanced translocation. (C) Hierarchical clustering of RNA-seq data placed the two CRTC1‑SS18-positive cases close to EWSR1‑CREB1-positive tumours. (D) NTRK1 expression from RNA-seq data. AFH/PPMS, angiomatoid fibrous histiocytoma/primary pulmonary myxoid sarcoma; CCCS, cutaneous clear cell sarcoma; CM-CT ,cutaneousmelanocytoma withCRTC1–TRIM11 fusion; BCR, BCOR-rearranged sarcoma; CD4, CIC–DUX4-positive sarcoma; EwS, Ewing sarcoma.

Figure 5. Biological analysis of the CRTC1–SS18 gene fusion. (A) Morphological analysis of CRTC1–SS18-expressing cells. CRTC1–SS18 fusion-positive clones were morphologically distinct from control HEK293 cells; the cytoplasmic component was small, with pronounced
vacuoles and extended, thin pseudopodia (both images taken under phase contrast at ×200 magnification). (B) Expression of the CRTC1–SS18 fusion protein in HEK293 cells significantly increased anchorage-independent growth potential. The number of viable, colony-forming cells present, following incubation in soft agar, was increased 2.1-fold in HEK293 cells expressing CRTC1–SS18 as compared
with HEK293 cells transfected with a control plasmid. Viable cells were determined with a fluorometric assay. $p < 0.0001$, $t = 8.61$, degrees of freedom

(d.f.) = 14. Error bars represent standard error of the mean (SEM) (n = 8). (C) Expression of the CRTC1–SS18 fusion protein in HEK293 cells significantly increased cell migration. The number of HEK293 cells expressing CRTC1–SS18 that migrated through 8-μm pores in a Boyden chamber assay in 16 h was significantly increased as compared with HEK293 cells transfected with a control plasmid.
This was apparent by inspection by microscopy (at ×4objective magnification) and by a colourimetric assay. $p < 0.0001$, t = 6.2.2, d.f. = 38. Error bars show SEM (n = 20). (D) Expression of the CRTC1–SS18 fusion protein in HEK293 cells significantly increased cell invasive
potential. The number of HEK293 cells expressing CRTC1–SS18 that invaded through 8-μmporescoatedinabasement membrane matrix in 16 h was significantly increased as compared with HEK293 cells transfected with a control plasmid. Invasive cells were counted at ×40 objective magnification; the mean number of invasive cells was 2.6 times greater for CRTC1–SS18-expressing cells than for control cells.
$p < 0.0001$, t = 6.108, d.f. = 42. Error bars show SEM (n = 22). OD, optical density.

References

1. Machado I, Navarro S, Llombart-Bosch A. Ewing sarcoma and the new emerging Ewing-like sarcomas: (CIC and BCOR-rearranged-sarcomas). A systematic review. Histol Histopathol 2016; 31: 1169–1181.
2. Antonescu C. Round cell sarcomas beyond Ewing: emerging entities. Histopathology 2014; 64: 26–37.
3. Pierron G, Tirode F, Lucchesi C, et al. Anew subtype of bone sarcoma defined by BCOR–CCNB3 gene fusion. Nat Genet 2012; 44: 461–466.
4. Kawamura-Saito M, Yamazaki Y, Kaneko K, et al. Fusion between CIC and DUX4 up-regulates PEA3 family genes in Ewing-like sarcomas with t(4;19)(q35;q13) translocation. Hum Mol Genet 2006; 15: 2125–2137.
5. Antonescu CR, Owosho AA, Zhang L, et al. Sarcomas with CIC-rearrangements are a distinct pathologic entity with aggressive outcome: a clinicopathologic and molecular study of 115 cases. Am JSurgPathol2017; 41: 941–949.
6. Puls F, Niblett A, Marland G, et al. BCOR–CCNB3 (Ewing-like) sarcoma: a clinicopathologic analysis of 10 cases, in comparison with conventional Ewing sarcoma. Am J Surg Pathol 2014; 38: 1307–1318.
7. Sugita S, Arai Y, Tonooka A, et al. AnovelCIC–FOXO4 gene fusion in undifferentiated small round cell sarcoma: a genetically distinct variant of Ewing-like sarcoma. Am J Surg Pathol 2014; 38: 1571–1576.
8. Specht K, Zhang L, Sung YS, et al. Novel BCOR–MAML3 and ZC3H7B–BCOR gene fusions in undifferentiated small blue round cell sarcomas. Am J Surg Pathol 2016; 40: 433–442.
9. Brohl AS, Solomon DA, Chang W, et al. The genomic landscape of the Ewing sarcoma family of tumors reveals recurrent STAG2 mutation. PLoS Genet 2014; 10: e1004475.
10. Nicorici D, Satalan M, Edgren H, et al. FusionCatcher – a tool for finding somatic fusion genes in paired-end RNA-sequencing data. bioRxiv 2014; https://doi.org/10.1101/011650 [Epub ahead of print].

11. Dobin A, Davis CA, Schlesinger F, et al. STAR: ultrafast universal RNA-seq aligner. Bioinformatics 2013; 29: 15–21.
12. Haas B, Dobin A, Stransky N, et al. STAR-Fusion: fast and accurate fusion transcript detection from RNA-seq. bioRxiv 2017; https://doi .org/10.1101/120295 [Epub ahead of print].
13. Ge H, Liu K, Juan T, et al. FusionMap: detecting fusion genes from next-generation sequencing data at base-pair resolution. Bioinformatics 2011; 27: 1922–1928.
14. Bray NL, Pimentel H, Melsted P, et al. Near-optimal probabilistic RNA-seq quantification. Nat Biotechnol 2016; 34: 525–527.
15. R Development Core Team. R: a Language and Environment for Statistical Computing. R Foundation for Statistical Computing: Vienna, 2017.
16. Cellier L, Perron E, Pissaloux D, et al. Cutaneous melanocytoma with CRTC1–TRIM11 fusion: report of 5 cases resembling clear cell sarcoma. Am J Surg Pathol 2018; 42: 382–391.
17. Conkright MD, Canettieri G, Screaton R, et al. TORCs: transducers of regulated CREB activity. Mol Cell 2003; 12: 413–423.
18. Iourgenko V, Zhang W, Mickanin C, et al. Identification of a family of cAMP response element-binding protein coactivators by genome-scale functional analysis in mammalian cells. Proc Natl Acad Sci U S A 2003; 100: 12147–12152.
19. Nordkvist A, Gustafsson H, Juberg-Ode M, et al. Recurrent rearrangements of 11q14–22 in mucoepidermoid carcinoma. Cancer Genet Cytogenet 1994; 74: 77–83.
20. Tonon G, Modi S, Wu L, et al. t(11;19)(q21;p13) translocation in mucoepidermoid carcinoma creates a novel fusion product that dis-rupts a Notch signaling pathway. Nat Genet. 2003; 33: 208–213.
21. Enlund F, Behboudi A, Andren Y, et al. Altered Notch signaling resulting from expression of a WAMTP1–MAML2 gene fusion in mucoepidermoid carcinomas and benign Warthin's tumors. Exp Cell Res 2004; 292: 21–28.
22. Tirado Y, Williams MD, Hanna EY, et al. CRTC1/MAML2 fusion transcript in high-grade mucoepidermoid carcinomas of salivary and thyroid glands and Warthin's tumors: implications for histogene-sis and biologic behavior. Genes Chromosomes Cancer 2007; 46: 708–715.
23. Middeljans E, Wan X, Jansen PW, et al. SS18 together with animal-specificfactorsdefines human BAF-type SWI/SNF com-plexes. PLoS One 2012; 7: e33834.
24. Clark J, Rocques PJ, Crew AJ, et al. Identification of novel genes, and SSX, involved in the t(X;18)(p11.2;q11.2) translocation found in human synovial sarcoma. Nat Genet 1994; 7: 502–508.
25. Skytting B, Nilsson G, Brodin B, et al. A novel fusion gene, SYT–SSX4, in synovial sarcoma. JNatl CancerInst 1999; 91: 974–975.
26. Nielsen TO, Poulin NM, Ladanyi M. Synovial sarcoma: recent dis-coveries as a roadmap to new avenues for therapy. Cancer Discov 2015; 5: 124–134.
27. Schram AM, Chang MT, Jonsson P, et al. Fusions in solid tumours: diagnostic strategies, targeted therapy, and acquired resistance. Nat Rev Clin Oncol 2017; 14: 735–748.

Figure1

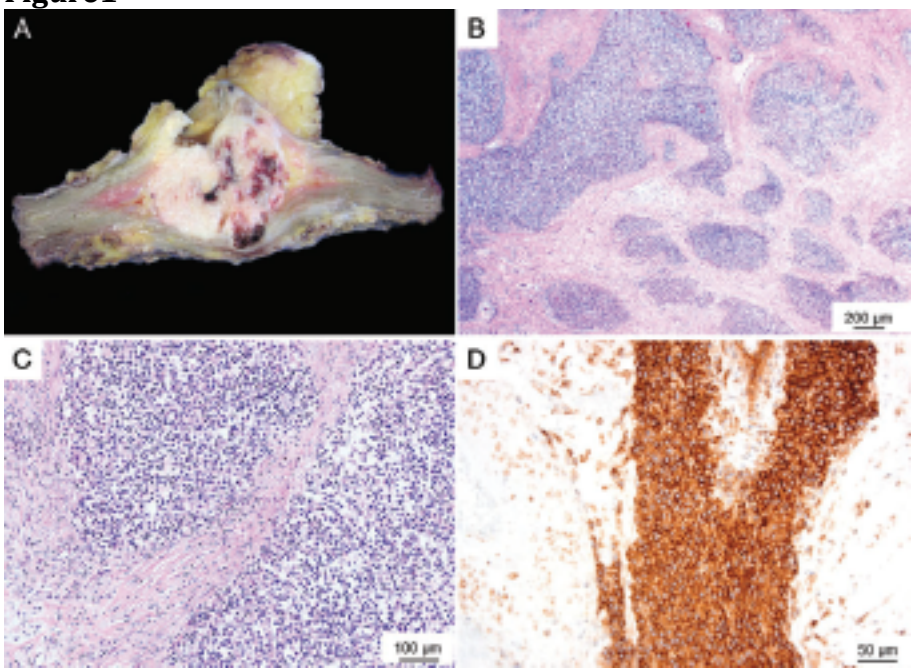

Figure 2

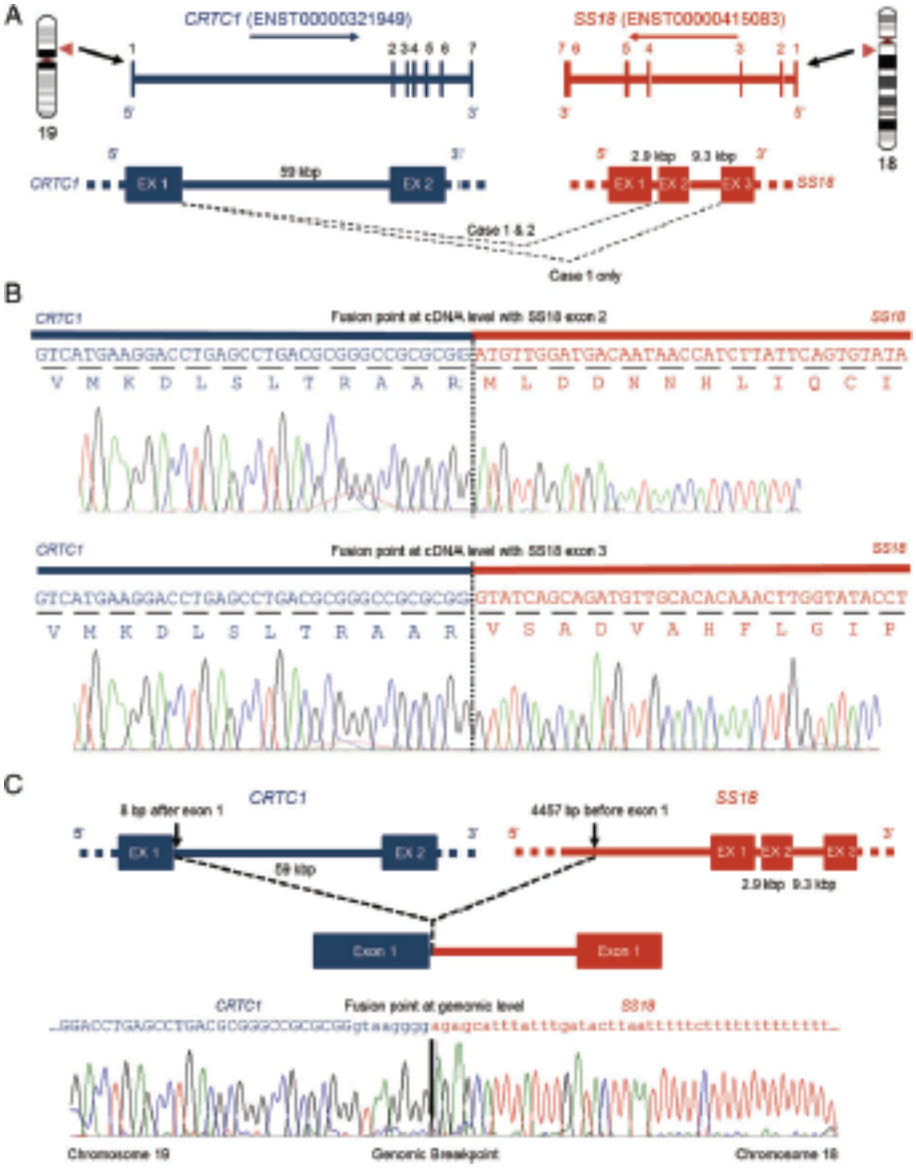
A
CRTC1 (ENST00000321949)
SS18 (ENST00000415083)
19
18
CRTC1
EX 1
EX 2
59 kbp
SS18
2.9 kbp
9.3 kbp
Case 1 & 2
Case 1 only
B
Fusion point at cDNA level with SS18 exon 2
Fusion point at cDNA level with SS18 exon 3
C
8 bp after exon 1
4457 bp before exon 1
Exon 1
Exon 1
Fusion point at genomic level
Chromosome 19
Genomic Breakpoint
Chromosome 18

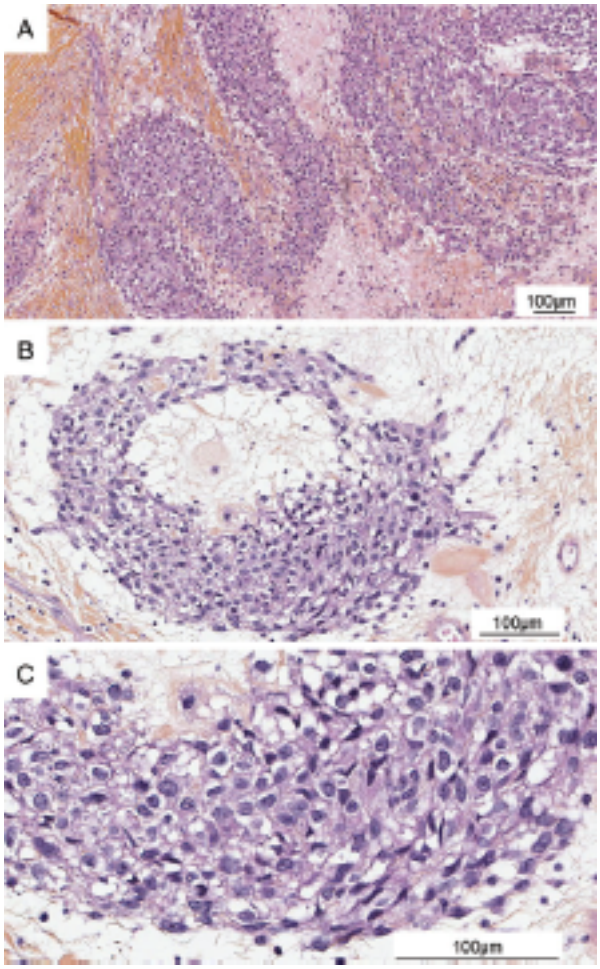

Figure 3

Figure 4

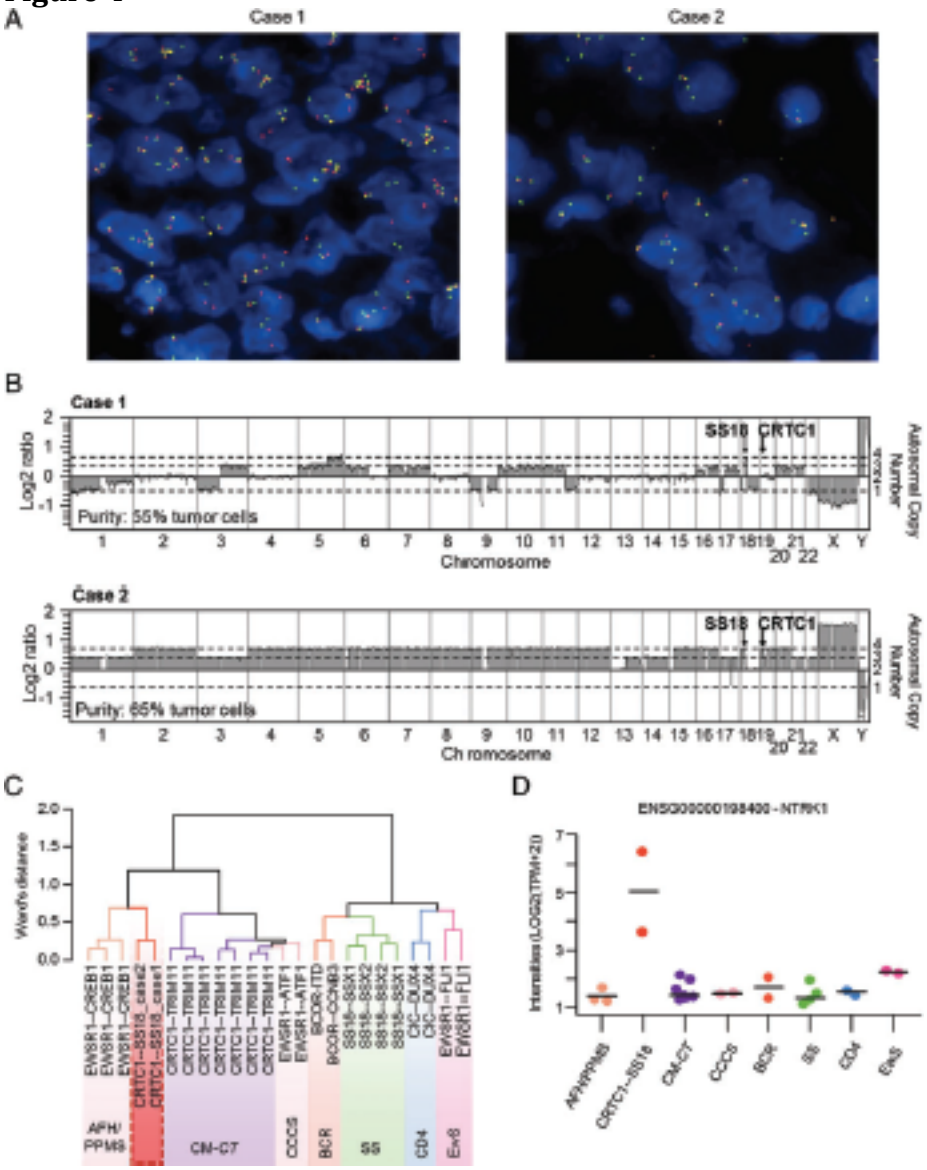
A
Case 1
Case 2
B
Case 1
Log2 ratio
SS18
CRTC1
Purity: 55% tumor cells
Chromosome
Autosomal Copy Number
Case 2
Purity: 65% tumor cells
C
Ward's distance
AFH/PPMS
CIN-C7
CCCS
BCR
SS
CD4
Ex6
D
ENSG00000198400 - NTRK1
Intensities (LOG2(TPM+20))
AFH/PPMS
CRTC1–SS18
CIN-C7
CCCS
BCR
SS
CD4
Ews

Figure 5

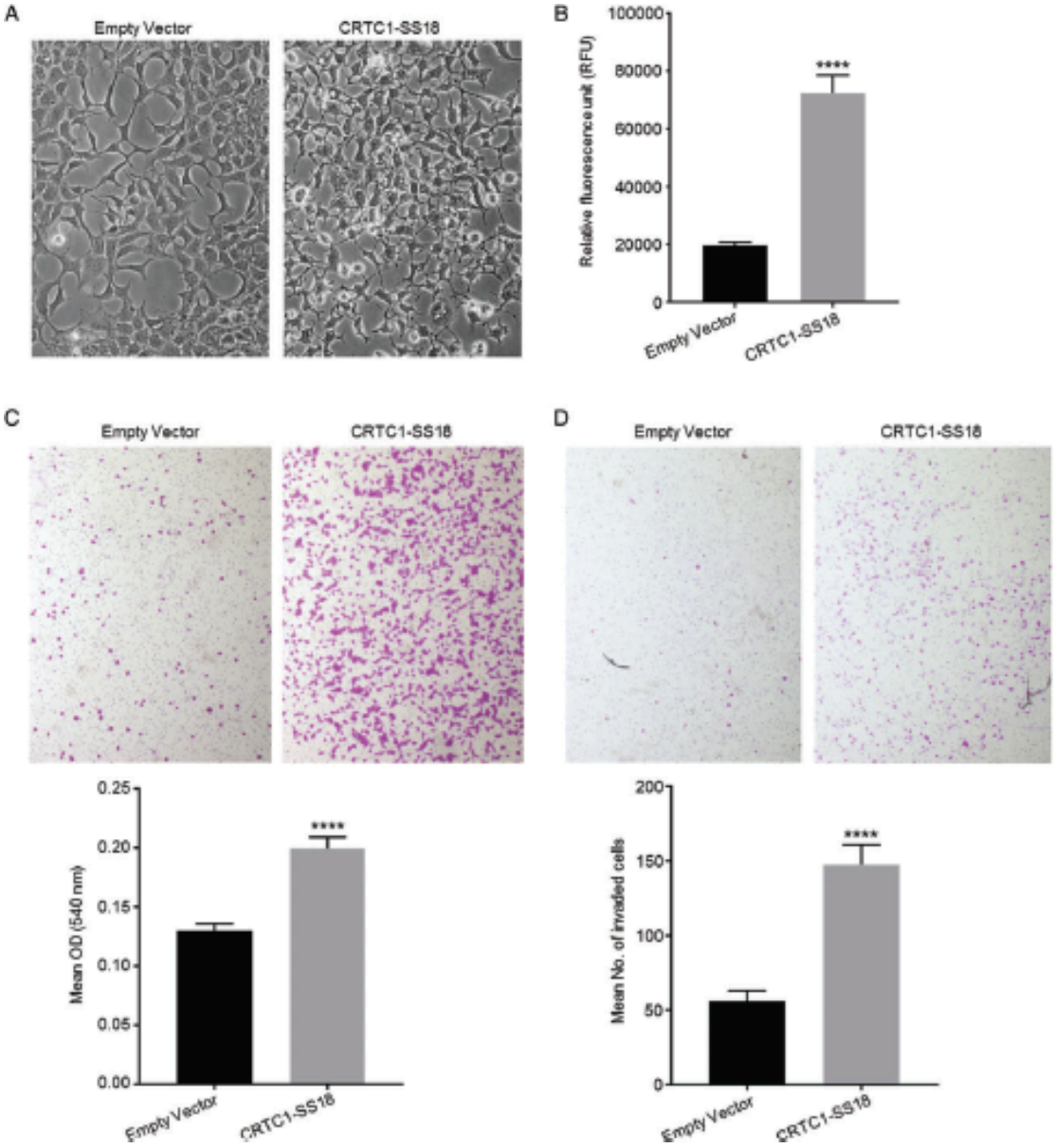
A
Empty Vector
CRTC1-SS18
B
Relative fluorescence unit (RFU)
100000
80000
60000
40000
20000
0
****
Empty Vector
CRTC1-SS18
C
Empty Vector
CRTC1-SS18
Mean OD (540 nm)
0.25
0.20
0.15
0.10
0.05
0.00
****
Empty Vector
CRTC1-SS18
D
Empty Vector
CRTC1-SS18
Mean No. of invaded cells
200
150
100
50
0
****
Empty Vector
CRTC1-SS18